

Experimental confirmation of the atomic force microscope cantilever stiffness tilt correction

Richard S. Gates

Citation: *Review of Scientific Instruments* **88**, 123710 (2017);

View online: <https://doi.org/10.1063/1.4986201>

View Table of Contents: <http://aip.scitation.org/toc/rsi/88/12>

Published by the *American Institute of Physics*



Scilight

Sharp, quick summaries **illuminating**
the latest physics research

Sign up for **FREE!**

AIP
Publishing

Experimental confirmation of the atomic force microscope cantilever stiffness tilt correction

Richard S. Gates

Nanomechanical Properties Group, National Institute of Standards and Technology, 100 Bureau Drive, STOP 8370, Gaithersburg, Maryland 20899, USA

(Received 2 June 2017; accepted 21 November 2017; published online 14 December 2017)

The tilt angle (angle of repose) of an AFM cantilever relative to the surface it is interrogating affects the effective stiffness of the cantilever as it analyzes the surface. For typical AFMs and cantilevers that incline from 10° to 15° tilt, this is thought to be a 3%–7% stiffness increase correction. While the theoretical geometric analysis of this effect may have reached a consensus that it varies with $\cos^{-2}\theta$, there is very little experimental evidence to confirm this using AFM cantilevers. Recently, the laser Doppler vibrometry thermal calibration method utilized at NIST has demonstrated sufficient stiffness calibration accuracy, and precision to allow a definitive experimental confirmation of the particular trigonometric form of this tilt effect using a commercial microfabricated AFM cantilever specially modified to allow strongly tilted (up to 15°) effective cantilever stiffness measurements. <https://doi.org/10.1063/1.4986201>

INTRODUCTION

Atomic force microscopes (AFMs) utilize microfabricated cantilevers to image and measure properties of surfaces at the nanometer scale. These cantilevers are inclined at small angles (usually around 10° – 15°) to allow the tips of the cantilevers to access the sample surface without the cantilever holder making contact. For imaging, it is important to know the approximate force applied to the surface by the cantilever to avoid damaging the surface or excessively wearing the tip. In some cases, researchers are interested in quantitatively interrogating the surface (for example, to determine adhesion and other nanomechanical properties), and in these cases, it is necessary to accurately know the stiffness of the cantilever. This can be determined by a suitable calibration method. Since the tilt of the cantilever will affect the operative or effective stiffness of the cantilever in the AFM, the tilt correction factor should be known for accurate results.

Early efforts to calibrate the spring constants of AFM cantilevers in the 1990s were focused on approximate calibrations with repeatability in the $\pm 10\%$ to $\pm 30\%$ range, so smaller influences on the overall uncertainty were often glossed over. The geometric effect of a tilted cantilever, for example, was sometimes ignored as demonstrated by the oversimplification of apparatus representation where cantilevers are depicted as horizontal.^{1,2} Even when it is mentioned or shown that the cantilever is tilted, some of the essential bookkeeping that adequately describes the appropriate relationship is often missing. In some cases, the computational detail itself is missing.³ In other papers, the terminology is vague⁴ and can easily be misunderstood or misinterpreted. The main issue revolves around whether or not the calibration included any tilt effect, so it is important to properly define the key terms and how they are related.

There are two flexural spring constants associated with typical AFM cantilever use as shown in Fig. 1. The “intrinsic”

spring constant, k_i , is the fundamental stiffness perpendicular to the long axis of the cantilever. This value is also the stiffness reported by cantilever manufacturers for their products.

The operative or “effective” cantilever stiffness is the value, k_e , perpendicular to the (horizontal) sample surface. This is the value ultimately important to the AFM manufacturers and the user community since it defines the actual forces being applied to the surface during use and the angle can be different for different manufacturers and different models of AFMs (i.e., it is instrument specific). The geometric correction factor between these two spring constants was in dispute initially due mainly to some confusion from early publications that provided inconsistent geometric analyses^{5–8} which ranged from no correction to multiplying by $\cos\theta$ to dividing by $\cos\theta$. Current consensus indicates that the geometric relationship between effective and intrinsic spring constants should be \cos^{-2} as noted by Attard *et al.*,⁹ Heim *et al.*,¹⁰ Hutter,¹¹ and Gates and Reitsma,¹²

$$k_e = \frac{k_i}{\cos^2\theta}. \quad (1)$$

It is important to know which version of the cantilever spring constant is meant since different cantilever calibration methods provide different ones. Euler-Bernoulli (dimensional) modeling, Cleveland added mass,¹³ Sader resonance/dissipation,¹⁴ and laser Doppler vibrometry (LDV) thermal calibration¹⁵ methods typically directly provide the “intrinsic” spring constant. The reference cantilever⁴ and AFM thermal calibration¹⁶ methods typically directly provide the “effective” spring constant. If the tilt angle is known for an instrument, these values can become interchangeable with the proper tilt correction factor. Early attempts to *experimentally* validate a relationship between the tilt angle and effective cantilever stiffness were attempted by Heim in 2004¹⁰ through a series of AFM adhesion experiments, but despite covering a large angle range of 0° – 35° , the large data scatter (a range of perhaps $\pm 50\%$ at each

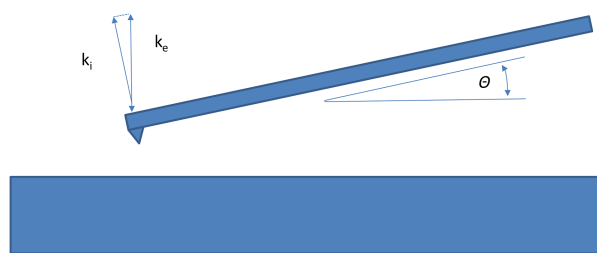


FIG. 1. AFM cantilever tilt effect on the spring constant.

angle) was credible for indicating little more than an increasing effective stiffness with angle.

This study was designed to experimentally verify the actual cantilever effective stiffness-tilt relationship accurately and precisely enough to properly resolve the appropriate model form. It utilized a specially modified colloid probe cantilever and the LDV thermal calibration method for colloid probe cantilevers recently developed at NIST¹⁷ to accurately measure the effective spring constant of the cantilever as a function of cantilever tilt angle. The data were then fit to a generalized power law model to verify the form of the stiffness dependence on tilt angle.

EXPERIMENT DESIGN

Experimental validation of the form of the angle tilt correction requires an accurate and precise calibration method and a means of applying the method to real AFM cantilevers under a range of tilt angles. Recent advancement at NIST in the calibration of static stiffness of AFM cantilevers using a laser Doppler vibrometry thermal method have demonstrated that uncertainties near 1% could be achieved. This was first shown with ideal rectangular cantilevers,¹⁵ then with tipped cantilevers of different shapes,¹⁸ and finally with colloid probe cantilevers with spheres attached.¹⁷ One particularly beneficial aspect of the work on the colloid probe cantilevers was the observation that using *small* spheres seemed to have a stabilizing influence on the sample beam drift during LDV data acquisition, resulting in lower measurement uncertainty. The effect was thought to occur due to the ability of small spheres

to reflect a subset of the original laser sample beam spot that is locked to the apex of the sphere as shown in Fig. 2. Typically [Fig. 2(a)], a beam can drift slightly laterally relative to the sample surface during long signal acquisition (1–2 min). Since LDV thermal calibration measurements provide the stiffness of the cantilever at the exact point of the laser spot and stiffness varies along the length of the cantilever approximately as a cubic, even small 1% changes in laser spot length location can have a significantly larger 3% effect on the final calibrated stiffness. As a result, accuracy and precision of the measurement can suffer. When a small sphere is used instead [Fig. 2(b)], the physical location of the reflected beam is locked onto the apex of the sphere even if the sample beam or surface drifts laterally with time, thus stabilizing the signal and enhancing calibration accuracy and precision.

A second requirement for calibrating the spring constant of a cantilever in the NIST LDV instrument is the ability to get a proper reflection from both a sample laser spot (at the end of the cantilever where the spring constant is desired) and a reference laser spot (located at the base of the cantilever, usually on the handle chip). This is easily accomplished when the cantilever is flat, reflective, and horizontal so that the beams can easily reflect back into the lens for detection. A tilt of a few degrees starts to produce measurable decreases in the reflected signal intensity, so tilting to realistic angles typical of an AFM (up to 15°) would result in total signal loss. This issue can be solved by utilizing a colloid probe cantilever and gluing a second reflective gold sphere to the base of the cantilever as shown in Fig. 3. In this way, both sample and reference beams have a spherical surface to reflect from and signal intensities can be maintained even at high cantilever tilt angles. For the purposes of stiffness calibration, the *reference* beam location is not position sensitive, so the stabilization effect of a small sphere is *not* required.

A third requirement for the experiment is to try to minimize the difference in the focal depth of the sample and reference surfaces. If one of the surfaces is too out-of-focus, then the signal intensity suffers and calibration precision is reduced. For this reason, a much larger sphere needs to be chosen for the base (reference) surface such that the tops of the spheres are co-planar (i.e., simultaneously in focus) at about half of the 15° tilt range.

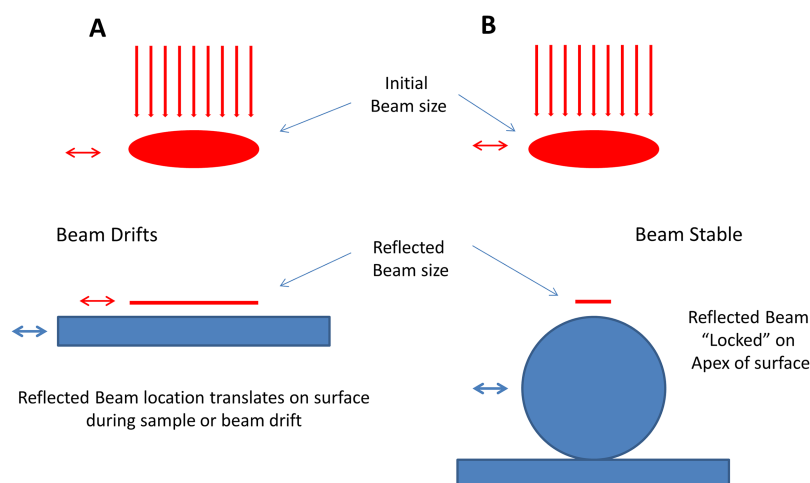


FIG. 2. Sample beam lateral drift stabilization using small spheres.

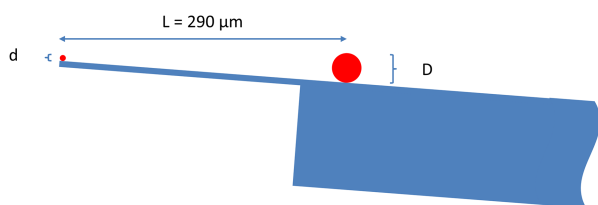


FIG. 3. Side view schematic for the tilt experiment cantilever.

An estimation of the base sphere size (D) required for a series of experiment for a $230\ \mu\text{m}$ long colloid probe cantilever with a $6\ \mu\text{m}$ diameter sphere (d) at the tip, inclined at 7.5° and set back about $60\ \mu\text{m}$ on the handle chip indicated that a nominal $44\ \mu\text{m}$ diameter sphere would be needed.

EQUIPMENT

The test cantilever consisted of a commercial colloid probe cantilever (SQube²⁰ CP-FM-Au-C, Nanosensors, Bickelbach, Germany) with a $6\ \mu\text{m}$ diameter gold sphere pre-attached at the end. A $44\ \mu\text{m}$ diameter gold sphere was selected from a commercial source batch (Alfa Aesar #43900, Ward Hill, MA) and glued near the base of the cantilever (Setback $66\ \mu\text{m}$) using a UV cure adhesive (Bug-Bond Lite, UK) as shown in Fig. 4. Accurate control of the cantilever tilt was achieved using a 15° small goniometer stage (Thorlabs GN-05, Newton, NJ) with a vernier scale capable of angular uncertainty better than 0.2° .

LDV thermal calibration measurements were conducted using the NIST MSA-500 system (Polytec, Germany) described in detail in a previous publication.¹⁵

The general experimental procedure for determining the spring constant of a cantilever using the LDV thermal calibration method consists of focusing the LDV sample laser spot on the location on the cantilever where one wishes to know the flexural stiffness and acquiring a thermal vibrational spectrum.

A reference laser spot placed on the chip at the base of the cantilever serves to background-subtract the vibration of the

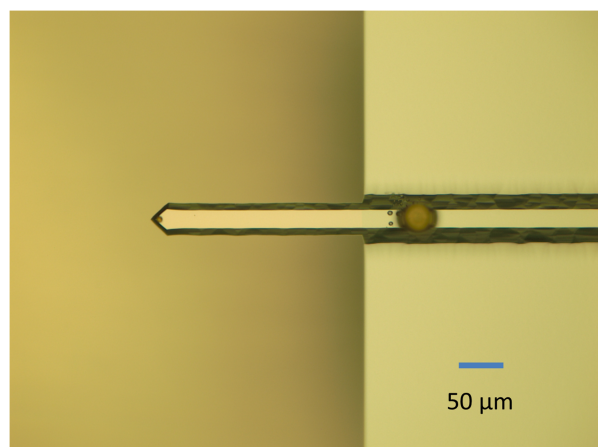


FIG. 4. Top view optical micrograph of the tilt experiment cantilever with a large sphere attached at the base.

chip itself. The cantilever has a natural flexural resonance frequency that forms a peak in the spectrum. The size of the peak represents the “springiness” of the cantilever. The area under the resonance peak of the power spectral density spectrum is measured by fitting it to a Lorentzian model and is converted to the spring constant through the equipartition theorem as described in detail previously.^{15,18}

RESULTS AND DISCUSSION

The test cantilever chosen for the tilt experiment was initially calibrated prior to adding the large base sphere using the colloid probe LDV thermal method described previously.¹⁷ The mode correction factor (needed to convert from the first flexural mode dynamic stiffness measured in the LDV to static stiffness) was experimentally measured as 0.981 based on the first three resonance modes of the cantilever.¹⁸ A series of 5 repeat LDV thermal calibrations determined the baseline (0° tilt) measured values of the resonance frequency ($f_0 = 69.45 \pm 0.01\ \text{kHz}$ ²¹), quality factor ($Q = 190 \pm 11$), and stiffness ($k_i = 2.620 \pm 0.015\ \text{N/m}$) for this cantilever. Note that for this particular baseline case there is no tilt and $k_i = k_e$.

A series of LDV thermal calibration tilt experiments were conducted on the modified (large base sphere added) cantilever over three different days, and the repeat results statistically averaged to provide reasonably good precision. Each experiment consisted of aligning the goniometer at the selected angle and then placing the cantilever under the LDV optics, oriented such that the larger reference sphere was along the right edge of the field of view of the optics with the tip end near the middle of the field. Adjustments were then made to the focus (to be on the tip sphere) and iteratively optimizing both the sample beam location (on the tip sphere) and reference beam location (on the base sphere) to maximize the signal intensity. For most angles, the optimized peak intensity was 100%. At the highest angle (15°), the maximum signal intensity dropped slightly to about 90% due to the focal depth of field mismatch; however, repeatable cantilever calibration values are easily achieved with LDV

TABLE I. LDV thermal calibration measured effective stiffness at varying tilt angles. LDV acquisition parameters: 20 \times lens ($2.5\ \mu\text{m}$ spot size), 100 kHz bandwidth, 128 000 FFT, 400 scans.

Inclined angle			Effective stiffness, k_e		
θ (deg)	$\cos \theta$	\pm	Average (N/m)	\pm (N/m)	\pm (%)
0	1.0000	6.1×10^{-6}	2.617	0.023	0.9
5	0.9962	0.000 31	2.661	0.042	1.6
7	0.9925	0.000 43	2.665	0.024	0.9
9	0.9877	0.000 55	2.691	0.028	1.0
10	0.9848	0.000 61	2.723	0.024	0.9
11	0.9816	0.000 67	2.722	0.060	2.2
12	0.9781	0.000 73	2.754	0.035	1.3
13	0.9744	0.000 79	2.777	0.026	1.0
14	0.9703	0.000 85	2.785	0.032	1.2
15	0.9659	0.000 91	2.822	0.023	0.8
			Average		1.2

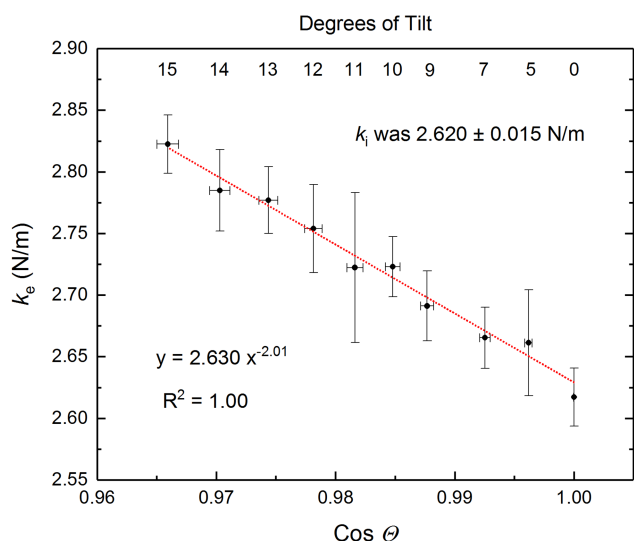


FIG. 5. Power law model data fit for the cantilever tilt experiment.

signals above 75% intensity. At least six repeat analyses were conducted at each tilt angle. Since the cosine function is non-linear and does not change much at small angles, the tilt angle step sizes were larger near zero degrees and smaller at higher angles near 15° . This provided better data uniformity on the x-y data plot. The data are summarized in Table I.

The uncertainties in the effective stiffness (k_e) measurements were typically near $\pm 1\%$. A couple of data points (5° and 11° tilt) had slightly higher uncertainties, and this was thought to be due to slight imperfections in the surface reflectivity of the spheres at those particular angles. It should be noted that the zero tilt measurement with the large base sphere attached ($k_e = k_i$ value of 2.617 ± 0.023 N/m) from Table I is indistinguishable from the same zero tilt measurement made prior to attaching the large base sphere ($k_i = 2.620 \pm 0.015$ N/m) which implies that there is no significant effect of using a large sphere for reflecting the reference beam, on the accuracy of the measured stiffness of the cantilever using the LDV thermal technique.

Rather than a simple linear plot of k_e vs $\cos^{-2} \theta$ and seeing if the slope of the linear fit was equivalent to the intrinsic cantilever stiffness k_i , a more revealing method is to plot the data as a power law and let both the pre-exponential and exponent terms float as unknowns to see how close they come to anticipated values of k_i and -2 in the fit. The data were plotted as k_e vs $\cos \theta$ as shown in Fig. 5 and fitted to a power law function as $k_e = A * \cos^n \theta$ using the k_e and $\cos \theta$ data weighted by the k_e and $\cos \theta$ uncertainties provided in Table I and shown in Fig. 5. The data fit quite well ($R^2 = 1.00$) and specify that the pre-exponential (A) fit value is 2.630 ± 0.006 N/m which is statistically indistinguishable from the original baseline zero tilt k_i value of 2.620 ± 0.015 N/m prior to adding the large sphere at the base as well as the zero tilt k_e value of 2.617 ± 0.023 N/m with the sphere added (Table I). The fitted power exponent (n) is -2.01 ± 0.10 which experimentally confirms the hypothesized form shown in Eq. (1).

It should be noted that while the tilt angle stiffness correction is a significant contribution to the representation of accurate forces between the cantilever and surface in an AFM, there are other contributions that may need to be considered. For example, long tips and large colloid spheres on the ends of cantilevers can also contribute to the need for an additional geometric correction as noted by Heim *et al.*¹⁰ and Edwards *et al.*¹⁹

CONCLUSIONS

An experiment was designed to leverage the capabilities of the NIST LDV thermal calibration method for colloid probe cantilevers in order to accurately measure the effect of the cantilever tilt angle on cantilever effective stiffness. The relationship between cantilever effective stiffness and the inclined angle has been experimentally verified using a microfabricated AFM cantilever as $\cos^{-2} \theta$.

ACKNOWLEDGMENTS

The author would like to thank Dr. Jon Pratt at NIST for his thoughtful comments on a previous LDV thermal calibration paper, which triggered the idea for how to design a special process to accurately and experimentally measure the tilt angle contribution to cantilever effective stiffness.

- 1 A. Torii, M. Sasaki, K. Hane, and S. Okuma, *Meas. Sci. Technol.* **7**(2), 179–184 (1996).
- 2 C. T. Gibson, G. S. Watson, and S. Myhra, *Nanotechnology* **7**(3), 259–262 (1996).
- 3 H. S. Kim and P. J. Bryant, *J. Vac. Sci. Technol., A* **11**(4), 768–772 (1993).
- 4 E. L. Florin, V. T. Moy, and H. E. Gaub, *Science* **264**(5157), 415–417 (1994).
- 5 M. Tortonese and M. Kirk, *Proc. SPIE* **3009**, 53–60 (1997).
- 6 P. J. Cumpson and J. Hedley, *Nanotechnology* **14**(12), 1279–1288 (2003).
- 7 P. J. Cumpson, J. Hedley, and P. Zhdan, *Nanotechnology* **14**(8), 918–924 (2003).
- 8 P. J. Cumpson, C. A. Clifford, and J. Hedley, *Meas. Sci. Technol.* **15**(7), 1337–1346 (2004).
- 9 P. Attard, A. Carambassis, and M. W. Rutland, *Langmuir* **15**(2), 553–563 (1999).
- 10 L. O. Heim, M. Kappl, and H. J. Butt, *Langmuir* **20**(7), 2760–2764 (2004).
- 11 J. L. Hutter, *Langmuir* **21**(6), 2630–2632 (2005).
- 12 R. S. Gates and M. G. Reitsma, *Rev. Sci. Instrum.* **78**(8), 086101 (2007).
- 13 J. P. Cleveland, S. Manne, D. Bocek, and P. K. Hansma, *Rev. Sci. Instrum.* **64**(2), 403–405 (1993).
- 14 J. E. Sader, J. W. M. Chon, and P. Mulvaney, *Rev. Sci. Instrum.* **70**(10), 3967–3969 (1999).
- 15 R. S. Gates and J. R. Pratt, *Nanotechnology* **23**(37), 375702 (2012).
- 16 H. J. Butt and M. Jaschke, *Nanotechnology* **6**(1), 1–7 (1995).
- 17 R. S. Gates, W. A. Osborn, and G. A. Shaw, *Nanotechnology* **26**(23), 235704 (2015).
- 18 R. S. Gates, W. A. Osborn, and J. R. Pratt, *Nanotechnology* **24**(25), 255706 (2013).
- 19 S. A. Edwards, W. A. Ducker, and J. E. Sader, *J. Appl. Phys.* **103**(6), 064513 (2008).
- 20 Certain commercial equipment, instruments, or materials are identified in this paper to adequately specify the experimental procedure. Such identification does not imply recommendation or endorsement by the National Institute of Standards and Technology, nor does it imply that the materials or equipment identified are necessarily the best available for the purpose.
- 21 Unless otherwise specified, uncertainties expressed in this paper are ± 1 standard deviation and relative uncertainties are ± 1 standard deviation/mean and given in %.